The Astrophysical Journal, 700:1750–1758, 2009 August 1 doi:10.1088/0004-637X/700/2/1750

STEADY AND TRANSIENT RADIO EMISSION FROM ULTRACOOL DWARFS

Rachel A. Osten[1,6,7], N. Phan-Bao[2], Suzanne L. Hawley[3], I. Neill Reid[4], and Roopesh Ojha[5]
[1] Astronomy Department, University of Maryland, College Park, MD 20742, USA; osten@stsci.edu
[2] Institute of Astronomy and Astrophysics, Academica Sinica, P.O. Box 23-141, Taipei 10617, Taiwan; pbngoc@asiaa.sinica.edu.tw
[3] Astronomy Department, Box 351580, University of Washington, Seattle, WA 98195, USA; slh@astro.washington.edu
[4] Space Telescope Science Institute, 3700 San Martin Drive, Baltimore, MD 21218, USA; inr@stsci.edu
[5] NVI/United States Naval Observatory, Washington, DC 20392-54200, USA; rojha@usno.navy.mil
Received 2008 March 21; accepted 2009 June 3; published 2009 July 16

ABSTRACT

We present the results of multi-frequency radio observing campaigns designed to elucidate the nature of radio emission from very low mass stars. We detect radio emission in an additional two epochs of the ultracool dwarf binary LP 349−25, finding that the observed emission is broad band and steady on timescales between 10 s and 10.7 hr, as well as on timescales of 0.6 and 1.6 years. This system is unusual for ultracool dwarfs with detectable radio emission, in exhibiting a lack of any large-scale variability, particularly the bursting (periodic or aperiodic) behavior exhibited by the other objects with detectable levels of radio emission. We explore the constraints that the lack of variability on long- and short-timescales, and flat spectral index, imply about the radio-emitting structures and mechanism. The temporal constraints argue for a high latitude emitting region with a large inclination so that it is always in view, and survives for at least 0.6 years. Temporal constraints also limit the plasma conditions, implying that the electron density be $n_e < 4 \times 10^5$ cm^{-3} and $B < 130$ G in order not to see time variations due to collisional or radiative losses from high-energy particles. The observations and constraints provided by them are most compatible with a nonthermal radio emission mechanism, likely gyrosynchrotron emission from a spatially homogeneous or inhomogeneous source. This indicates that, similar to behaviors noted for chromospheric, transition region, and coronal plasmas in ultracool dwarfs, the magnetic activity patterns observed in active higher mass stars can survive to the substellar boundary. We also present new epochs of multi-frequency radio observations for the ultracool dwarfs 2MASS 05233822−140322 and 2MASS14563831−2809473(=LHS 3003); each has been detected in at least one previous epoch but are not detected in the epochs reported here. The results here suggest that magnetic configurations in ultracool dwarfs can be long-lasting, and support the need for further radio monitoring using a simultaneous, multi-frequency observing approach.

Key words: radio continuum: stars – stars: activity – stars: coronae – stars: late-type

1. INTRODUCTION

It was initially expected that radio emission would not be detected in ultracool dwarf stars, given the evidence that the number of objects exhibiting magnetic activity past a spectral type of M7V was declining (Hawley et al. 1996; West et al. 2004) despite increasingly rapid rotation; this seemed to match expectations that the cool, dense, and globally neutral atmospheres (fractional ionizations $\leqslant 10^{-5}$; Mohanty et al. 2002) of ultracool dwarfs would be unable to sustain the kinds of magnetic stresses thought to operate in the atmospheres of solar-like dwarf stars (spectral types F, G, K, and early M; Mohanty et al. 2002). Reiners & Basri (2007) showed that large-scale fields can be maintained by detecting their effect on transitions in molecular absorption bands, but the fields' connection to the non-radiative heating is still questionable.

Since the discovery of radio emission from one of these objects (Berger et al. 2001), there have been two key findings: the overall number of radio-emitting ultracool dwarfs is relatively low, $\sim 10\%$ (Berger 2006) with a slight preponderance for objects of spectral type M9 to more commonly display detectable levels of radio emission (Phan-Bao et al. 2007); and there is a wide variety of behavior exhibited by those objects which have shown detectable levels of radio emission. Several objects have displayed pulsar-like behavior (Berger et al. 2005; Hallinan et al. 2006) with periods consistent with those inferred from rotational periods using radius and $v \sin i$ measurements; interpulse emission is observed but seems to be less circularly polarized. A few others show large increases in flux density, accompanied by large amounts of circular polarization (Burgasser & Putman 2005) while still others have been detected in one epoch and undetected in others (Antonova et al. 2007). Variability is at the core of these behaviors; even the same object observed multiple times at radio wavelengths shows disparate behaviors (Berger 2002; Hallinan et al. 2006, 2007; Berger et al. 2008).

As with higher mass stellar radio emission (Osten 2007) it is possible that more than one type of radio emission mechanisms could be operating in the coronae of very low mass dwarfs: one, associated with gyrosynchrotron emission, is incoherent and consists of steady and variable wide-band radio emission, with moderate circular polarizations and roughly flat spectra; the other type being a coherent mechanism, possibly cyclotron maser emission, which can be extremely variable, usually highly circularly polarized, and can have steep spectra. Osten et al. (2006) attributed the steady radio emission from one ultracool dwarf to gyrosynchrotron emission based on its spectral index and circular polarization behaviors. The dramatic radio variability which has been observed on a few very low mass objects generally includes highly circularly polarized emission and points to a different radio emission mechanism than usually invoked for higher mass stellar radio emission, probably coherent. Current speculations are that it may be

[6] Hubble Fellow.
[7] Currently at Space Telescope Science Institute, 3700 San Martin Drive, Baltimore, MD 21218, USA.

cyclotron maser emission (Hallinan et al. 2007). Still unknown is how the source population of accelerated particles which produces this emission originates.

Although transition region and X-ray observations detect persistent fluxes from very low mass stars at levels compatible with scaling laws (based on Hα) extrapolated from earlier type M dwarfs, very low mass dwarfs appear to violate another tight relationship between magnetic activity indicators, namely, the X-ray luminosity–radio luminosity correlation pointed out by Güdel & Benz (1993) and Benz & Güdel (1994). The detection of both persistent and flaring radio emission from a handful of late M and L objects, reported in Berger et al. (2001) and Berger (2006), suggests that nonthermal radio emission is much stronger than predicted in some objects at late spectral types. The interpretation of the radio emission, however, is complicated by the fact that more than one potential mechanism may be at work: on the Sun and on other active stars, both incoherent and coherent nonthermal radio emissions produce detectable levels of radio emission (see, e.g., Dulk 1985; Güdel 2002). Detailed observations of solar radio emission show that a variety of emissions can be produced in the centimeter wavelength range depending on the type and location of emitting structures and their variation with time. Indeed, this provides a simple resolution to the apparent "violation" of the L_X–L_R relation in very low mass dwarfs noted by, e.g., Berger et al. (2005).

Studying stellar radio emission is important because it is the only wavelength region in which direct evidence of the role of accelerated electrons in stellar atmospheric structures and dynamics can routinely and easily be seen. In order to make advances in knowledge about atmospheric structure and dynamics, temporal and spectral information is needed. Detection epochs typically concentrate on building up exposure time at a single frequency with on-source times sufficient only to see very short timescale variability such as bursting behavior. Longer on-source times can probe rotationally induced variability as well as increase the likelihood of observing flares. Simultaneous multi-frequency radio observations are better at pinning down the emission mechanism and allowing for spectral–temporal modeling to better understand the emitting structures. To this end, we selected several objects which had been previously detected at a single radio frequency for follow-up with multi-frequency observations. The properties of the program sources are summarized in Table 1. The paper is organized as follows: Section 2 describes the properties of the program sources, Section 3 describes the observations, Section 4 discusses the data analysis and results, Section 5 provides a general discussion on how these observations contribute to our understanding of the nature of radio emission from very low mass stars, and Section 6 concludes what these data reveal about radio emission from ultracool dwarfs.

2. PROGRAM SOURCES

2.1. LP349−25

Gizis et al. (2000) recognized LP349−25 as a nearby star, deriving a spectral type of M8V with an estimated photometric distance of 8.3 pc. Close et al. (2002) observed the system with adaptive optics in an earlier epoch and found no evidence of multiplicity in images having spatial scales of 0.″13; however, Forveille et al. (2005) found clear evidence of the binary nature of the system using adaptive optics systems. The separation of the two stars was 0.125 ± 0.01 arcsec during the binarity discovery epoch; Gatewood et al. (2005) measured a parallax of 67.6 ± 2.0 mas for a distance estimate of 14.8 ± 0.4 pc. Based on this value, its M_J is 9.76. Forveille et al. (2005) estimated an orbital period of ∼five years. The infrared colors of Forveille et al. (2005) ($M_{K'} = 10.46$ for the companion, and $\Delta m_{K'} = 0.26 \pm 0.05$) lead to acceptable spectral type pairings of M7.5V+M8.5V or M8V+M9V. Phan-Bao et al. (2007) reported a single frequency detection at radio wavelengths from the binary; our team selected this object for follow-up observations at multiple wavelengths in order to characterize the nature of the radio emission and compare with behaviors displayed by other solar neighborhood ultracool dwarfs. Recent high-resolution spectroscopic observations with NIRSPEC on the Keck II telescope have determined a combined $v \sin i$ of the system to be ∼50 km s^{-1} (M. Rosa Zapatero Osorio 2007, private communication). Because of the small angular separation of the two stars, the spectrum obtained includes the contribution of both stars. The large $v \sin i$ measured thus could be due to the velocity separation of the two stars. However, if we assume that the estimated ∼five-year-period orbit is circular, then the small masses of the two components (≈0.09 $M_\odot$; Burgasser et al. 2007) imply that there would be a maximum orbital velocity amplitude of ∼20 km s^{-1}, and the excess velocity width could be due to rapid rotation. Thus, it may be possible that one or both of the two stars is rapidly rotating. Table 2 lists the image sensitivities of previously reported radio observations.

2.2. 2MASS J05233822−140322

This likely brown dwarf (hereafter designated 2M0523) was discovered by Cruz et al. (2003) and given an L2.5 spectral type. The derived distance was 13.4 ± 1.1 pc, implying M_J of 12.45. The distance is an estimate based on the spectral type and M_J calibration in the Cruz et al. paper. Photometric variations in the I band were probed by Koen (2005); the mean magnitudes in two runs ∼3 days apart agreed to within 0.01 mag, thereby providing no indication of infrared photometric variability. The first report on radio emission from this object was from Berger (2006), with a detection of 231 ± 13 μJy on one out of three occasions, and nondetections on the other two. Recently, Antonova et al. (2007) described additional single frequency radio observations which failed to detect the object at a level which is more than a factor of 10 lower than the detected flux density. Table 2 lists the image sensitivities of previously reported radio observations.

2.3. 2MASS J14563831−2809463=LHS 3003

LHS 3003 is a very low mass star with spectral type M7, at a distance of 6.56 ± 0.15 pc (Reid & Cruz 2002); its M_J is 11.00. Fuhrmeister et al. (2005) give a $v \sin i = 6 \pm 1.5$ km s^{-1}, noting asymmetric profiles of the Hα and Hβ emission lines, and a change in Balmer lines over several averaged spectra (without any photometric indication of flaring) as evidence for numerous active regions on the surface. Fleming et al. (1993) did not detect the source in *ROSAT* All-Sky Survey data, with an upper limit to the X-ray luminosity of $\log L_X$(erg s^{-1}) ⩽ 25.66. Schmitt et al. (1995) did detect the source with the *ROSAT* All-Sky Survey data with $\log L_X$(erg s^{-1}) of 26.27 (with apparently the same data set as Fleming et al. 1993). Mohanty & Basri (2003) give $v \sin i = 8$ km s^{-1}, $\log L_{\rm H\alpha}/L_{\rm bol} = -4.31$. Basri & Reiners (2006) looked at radial velocities to determine if this was a spectroscopic binary, and found no apparent variations in radial velocity. Reiners & Basri (2007) detected evidence for substantial large-scale magnetic field strengths on the surface,

Table 1
Properties of Program Sources

Source	Spectral Type	Distance (pc)	M_J	F_R (μJy)	λ_{obs} (cm)	Observation Date	Reference for F_R[a]	L_R (erg s^{-1} Hz^{-1})
LHS 3003	M7	6.2	11.0	270 ± 40	6	2002 May 2	BP05	1.2×10^{13}
LP349−25	M7.5V+M8.5V or M8V+M9V	14.8	9.76[b]	365 ± 16	3.6	2005 Dec 20	PB07	9.6×10^{13}
2M0523	L2.5	13.4	12.45	231 ± 13	3.6	2004 Jun 18	B06	5.0×10^{13}

Notes.
[a] PB07, Phan-Bao et al. (2007); B06, Berger (2006); BP05, Burgasser & Putman (2005).
[b] Combined value.

Table 2
Sensitivity of Past and Current Radio Observations of Program Sources

Date	λ_{obs} (cm)	$1\sigma_{rms}$[a] (μJy)	t_{exp} (hr)	Reference[b]
		LHS 3003		
1994 May 4	6	70	0.22	Current paper
1994 May 4	20	590	0.27	Current paper
2002 May 2	3.6	40	11	BP05
2002 May 2	6	40	11	BP05
2006 Jun 30	3.6	30	2.6	Current paper
2006 Jun 30	6	52	1.4	Current paper
2006 Jun 30	20	530	1.4	Current paper
		LP 349−25		
2005 Dec 20	3.6	16	1.7	PB07
2007 Jan 12	3.6	27	11.2	Current paper
2007 Jan 12	6	21	10.7	Current paper
2007 Aug 15	3.6	40	0.3	Current paper
2007 Aug 15	6	54	0.3	Current paper
		2M0523		
2004 May 3	3.6	16	1.6	B06
2004 May 17	3.6	20	1.7	B06
2004 Jun 18	3.6	13	2.1	B06
2006 Jun 30	3.6	19	6.2	Current paper
2006 Jun 30	6	36	3.0	Current paper
2006 Jun 30	20	118	3.4	Current paper
2006 Sep 23	3.6	15	9	A07

Notes.
[a] σ_{rms} was determined from blank regions of naturally weighted images.
[b] PB07, Phan-Bao et al. (2007); B06, Berger (2006); BP05, Burgasser & Putman (2005); A07, Antonova et al. (2007).

finding the product of magnetic field strength and filling factor to be $Bf = 1.6 \pm 0.2$ kG. Burgasser & Putman (2005) reported a detection of LHS 3003 at a wavelength of 6 cm in $\sim$11 hr with the Australia Telescope Compact Array (ATCA) at a flux density of 270 $\pm$ 40 μJy, while simultaneously obtained data at 3.6 cm with the same image noise did not reveal a detection. Table 2 lists the image sensitivities of previously reported radio observations.

3. OBSERVATIONS AND DATA REDUCTION

Our 2006 VLA[8] B-configuration observations were meant to further characterize the nature of the radio emission from LHS 3003 and 2M0523. In order to do this, we observed in two subarrays, one operating at 3.6 cm (4.8 GHz) and the other cycling between 6 and 20 cm (4.8, 1.4 GHz, respectively). We also extracted archival observations of LHS 3003 at 6 and 20 cm from the VLA archive and reduced those. C-configuration observations of LP349−25 in 2007 January were performed in two subarrays, each subarray recording one of two frequencies (3.6 or 6 cm). Additional A-configuration observations in 2007 August spanned roughly 20 minutes at each frequency, with data taken using the full configuration. All data were obtained in standard continuum mode with 50 MHz bandwidth.

[8] The National Radio Astronomy Observatory is a facility of the National Science Foundation operated under cooperative agreement by Associated Universities, Inc.

Table 3
Measured Flux Densities, Upper Limits for Reported Epochs

Source	λ (cm)	Flux Density or 3σ Upper Limit (μJy)
LHS 3003[a]	3.6	<90
”[a]	6	<156
”[a]	20	<1590
LP349−25[b]	3.6	383 ± 27
”[b]	6	320 ± 21
”[c]	3.6	262 ± 40
”[c]	6	338 ± 54
2M0523[a]	3.6	<57
”[a]	6	<108
”[a]	20	<354

Notes.
[a] Epoch of 2006 June 30; see Table 2.
[b] Epoch of 2007 January 12; see Table 2.
[c] Epoch of 2007 August 15; see Table 2.

After initial data reduction and imaging, no sources were found at the location of either LHS 3003 or 2M0523 at any frequency. We investigated and ruled out problems associated with EVLA antennas as factors in explaining the lack of detection. Correspondence of background sources in multiple epochs also lends reliability to the calibration and imaging steps. Table 2 compares the sensitivities of observations at all epochs for the three program sources, including other published radio observations. For 2M0523 and LHS 3003, the 1σ rms values from our observations are comparable to or less than those in the detection epochs at the corresponding frequency and should have detected the source if it were emitting at the same level as during the detection epoch. Our 3σ upper limits for the intensities of 2M0523 and LHS 3003 are listed in Table 3.

LP349−25 was detected at both frequencies at both epochs. Maps of the total intensity and circular polarization (Stokes V parameter) were made for the C- and A-configuration observations of LP349−25, first by including all visibilities and later after removing the contribution to the visibilities of background radio sources. Single Gaussian fits to the source position near phase center were done to determine position and peak flux density. Direct Fourier transforms of the visibilities at the position of the source were done to examine variability (AIPS task DFTPL). Table 3 lists the average radio flux density measurements or upper limits at each epoch and wavelength for our program sources. There was no significant level of circular

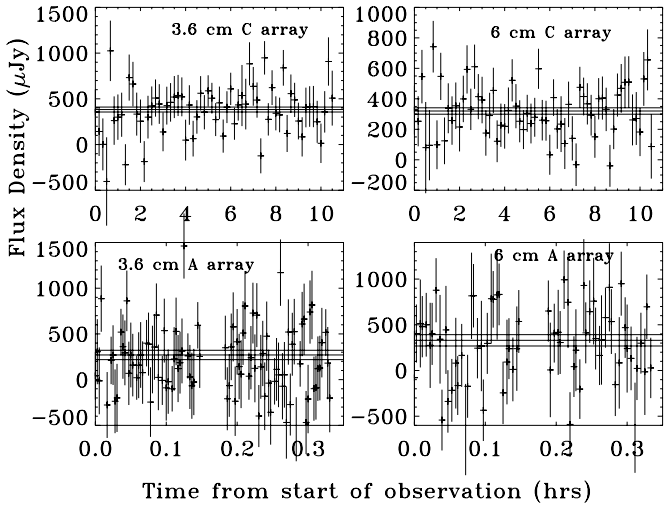

Figure 1. Detail of flux density variations for LP 349−25 from two different observing epochs, at 3.6 cm (8.4 GHz) and 6 cm (8.4 GHz). The solid line gives the average flux density and 1σ deviations; the crosses give individual measurements and error bars. For C-configuration observations the time binning is 10 minutes, and for A configuration it is 10 s. No bursting or periodic behavior is detectable.

polarization measured at any epoch, with 3σ upper limits of 78, 57 μJy at 3.6 and 6 cm in the C-configuration observation of LP349−25, respectively, and 120, 159 μJy at 3.6, 6 cm in A configuration, respectively.

4. DATA ANALYSIS AND RESULTS

In the following sections we describe the temporal and multi-frequency radio behavior for all three objects, in addition to the spatial resolution information provided by A-configuration observations of LP 349−25.

4.1. Temporal Behavior

The radio emission from LP349−25 shows steady levels over long-timescales. This is revealed by the similar flux densities in three epochs at 3.6 cm (Tables 1 and 3), identical to within 3σ based on differing exposure times and beam sizes. The time span of these 3.6 cm observations is 1.6 years. The 6 cm flux densities measured at two epochs are also consistent to within $<1\sigma$, over a time span of 0.6 years.

The intra-epoch behavior of LP 349−25 likewise reveals no detectable short-term variability. We investigated this using different techniques, designed to look for periodic signals and stochastic variability, either of which may appear at either frequency independently. We performed Lomb normalized periodograms on light curves of C-configuration data made at 10 s time resolution on both the 3.6 and 6 cm data to see if there was any evidence of periodic behavior in the radio emission, and found no statistically significant periodic signals. The time span of the data analyzed was 10.7 hr, with a maximum measurable period of 42 hr.

We also examined evidence for short-term aperiodic variability in both the C- and A-configuration observations of LP349−25. We computed the chi-squared value for the fit between the average flux density measured at 3.6 and 6 cm over the entire time interval, and the flux densities measured in finer time bins (10, 60, 300, and 600 s for the C-configuration observation, and 10 s for A-configuration observations). In all cases, the finer flux density variations were consistent with the average flux density. Figure 1 shows the flux density variability both between and within epochs for the C- and A-configuration observations of LP349−25.

The upper limits on radio emission from 2M0523 and LHS 3003 reflect variations of factors of 4 and 1.7, respectively, compared with the previously detected levels of radio emission. While the limits described in Antonova et al. (2007) for 2M0523 are much deeper, the addition of this extra epoch at which the radio emission is undetected lowers the fraction of time this object produces detectable levels of radio emission, to $\sim 10\%$. The previously described detected emission from LHS 3003, in Burgasser & Putman (2005), was accumulated over ~ 11 hr of integration, so the addition of this short epoch described here does not significantly affect the computed duty cycle of $\sim 87\%$. Further observations of this interesting source are required to study the transient nature of its radio emission.

4.2. Multi-Frequency Behavior

The detection epochs of LP349−25 and 2M0523 corresponded to only one wavelength (3.6 cm), and were reported in Phan-Bao et al. (2007) and Berger (2006), respectively. LHS 3003 was detected at 6 cm but not at simultaneously obtained 3.6 cm observations with the same sensitivity. While further multi-frequency observations of 2M0523 failed to detect the source at any wavelength, we have detected LP349−25 at both 6 and 3.6 cm on two occasions. Thus, only LP349−25 and LHS 3003 have constraints on the multi-frequency behavior of their radio emission. For radio flux density S_ν, $S_\nu \propto \nu^\alpha$, the 6–3.6 cm spectral index computed for LP349−25 from time-averaged C-configuration observations was $\alpha = 0.33 \pm 0.17$, and for the A-configuration observations it was $\alpha = -0.47 \pm 0.38$. We also computed α for time intervals within the C-configuration observation corresponding to the same time bins as done in Section 4.1 (10, 60, 300, and 600 s) and found no variability in α on these timescales. Burgasser & Putman (2005) reported the upper limit for the radio spectral index between 3.6 and 6 cm for LHS 3003 to be $\alpha \leqslant -1.2$. We note that for both LP349−25 and LHS 3003, the sensitivity in each frequency band for multi-frequency observations is very similar (numbers are listed in Table 2). In addition, the multi-frequency observations were made simultaneously in the case of LHS 3003 at the ATCA (both receivers operate at the same time), and the 2007 January 12 epoch for LP349−25. The 2007 August 15 epoch data of LP349−25 were obtained by alternating frequencies using the full array during the same observation session, so the multi-frequency information is not strictly simultaneous. Given the lack of variability on timescales $\geqslant$10 s described in Section 4.1, however, we can consider the multi-frequency recordings of LP 349−25 during the August 15 epoch to be simultaneous.

For LP349−25, the emission is stable at both frequencies in addition to being stable in time. This is revealed by the similar values returned for the radio spectral index at two epochs together with the lack of both short-term and long-term variability. The frequency difference between the 3.6 and 6 cm VLA receivers is $\Delta\nu = 3.6$ GHz, implying that the detected radio emission extends across this frequency range. In contrast, the emission from LHS 3003 reported in Burgasser & Putman (2005) was detected at only one wavelength at one epoch. This implies that the emission occurs over a range in frequency $\Delta\nu \leqslant 3.6$ GHz and possibly much smaller. Unfortunately, since the multi-frequency observations of LHS 3003 we performed on 2006 June 30 did not detect the source at any frequency, we cannot constrain the multi-frequency behavior of LHS 3003 during this epoch.

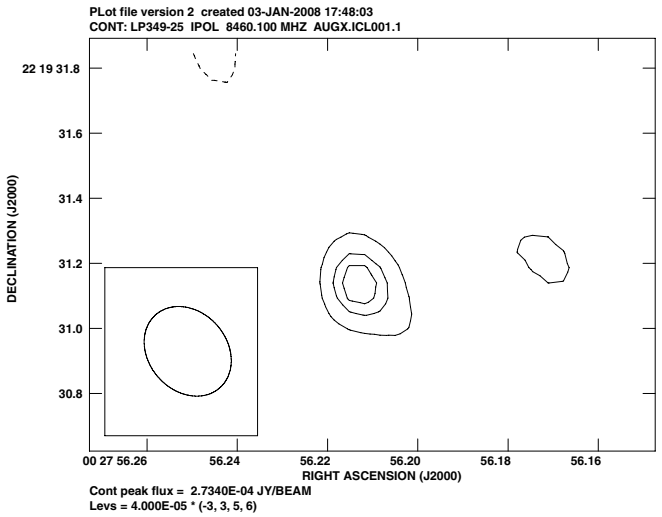

Figure 2. A-configuration VLA observations of the binary LP 349−25. The size of the radio beam is shown in the lower left corner. The 1σ rms from a blank region of the image is 40 μJy. The peak SNR in the source is only $\sim$6.7; it is not clear whether one or both dwarfs contributes to the radio emission. Details of the fit to the image contours are described in Section 4.3.

4.3. Imaging of LP349−25

We explored whether the contribution of both dwarfs to the radio emission from LP349−25 could be constrained from the observation made in A configuration. If the two dwarfs were at the separation noted during the discovery epoch (0.″125 ± 0.″01; Forveille et al. 2005) and had nearly equal intensity, we might have been able to separate the two components from our image of the A-configuration 3.6 cm data, made with 0.″047 pixel size. Two-dimensional elliptical Gaussian fits to the naturally weighted 3.6 cm A-configuration observations of LP349−25 return a major and minor axis of 0.36 ± 0.06 and 0.23 ± 0.04 arcsec, with a position angle measured north from east of 36° ± 14°. Deconvolving the fit from the clean beam, the nominal major and minor axes of the elliptical Gaussian are 0.″21 (minimum 0.″12, maximum 0.″28) and 0″ (minimum 0″ maximum 0.″09), with a position angle of 32° (minimum 1°, maximum 67°). Minimum and maximum values are the extrema obtained by a deconvolution of the source beam from the clean beam with 0.7 times the error of component values. Figure 2 shows a close-up of the radio contours. We explored using uniform or "super-uniform" weighting to enhance the longest baselines compared with the shortest ones, however these weighting schemes also increase the noise and these images produced peaks at lower significance value, with evidence for only one source at the location of LP349−25; there was no evidence for a second source out to the maximum distance sampled in the A-configuration image, 24″ from LP349−25. This is perhaps not surprising: the discovery epoch on 2004 July 3 of the binarity of LP349−25 (Forveille et al. 2005) revealed the separation between the two stars to be 0.″125 ± 0.″01 at a position angle of 12.°7 ± 2.°0 east from north, while an earlier epoch on 2001 September 18–19 (Close et al. 2002) showed the system to be unresolved. This earlier epoch occurred almost six years prior to our observations, and with the estimate by Forveille et al. (2005) that the orbital period is about five years an explanation for why the two stars were not resolved is apparent. The A-configuration observations thus do not constrain whether one or both dwarfs in the LP349−25 system contribute to the total observed radio emission; further observations at higher spatial resolution are needed to resolve the two dwarfs.

Spatially resolving the two stars in the binary system is important for two reasons. The first is that this will allow us to determine the relative amount of radio emission arising from each dwarf, and hence explore radio emission mechanisms further. As noted by Phan-Bao et al. (2007), the radio luminosity from the system is slightly higher than the steady levels seen from other radio-emitting ultracool dwarfs. The second lies in the unique nature of LP349−25 as a nearby tight binary with an orbital period amenable to astrometric monitoring; direct mass measurements are crucial to placing constraints on the formation processes of very low mass ($<$0.1 $M_{\odot}$) stellar objects (Burgasser et al. 2007). Mass determinations are also important for comparing with theoretically derived masses from evolutionary models, and establishing mass–luminosity relations in this mass range (Bouy et al. 2004). Due to the low flux density, sensitive high spatial resolution observations such as those attainable with the High Sensitivity Array are needed; we have an approved program to begin this monitoring, which should be able to attain an astrometric precision of $\approx$30 μas using phase referenced observations (Pradel et al. 2006). LP 349−25 thus provides the keys to understanding the formation of ultracool dwarfs as well as the enigmatic nature of their radio emission.

5. DISCUSSION

Of our observations of three ultracool dwarfs, the detections of LP 349−25 offer the most stringent constraints on the types of radio emission produced in ultracool dwarfs. The relevant and interesting facts about the radio behavior seen on LP 349−25 are that the emission is constant on both short- and long-timescales, and that the observed multi-frequency radio emission has a flat spectral index which also does not appear to vary on short- and long-timescales. This is unusual behavior in light of the fact that the few ultracool dwarfs which have been detected at radio wavelengths have all exhibited dramatic variability, whether periodic or bursting behavior. Here, we explore what constraints these details provide within the context of behavior seen on active stars and ultracool dwarfs.

5.1. Constraints from Absence of Short-Term Variability

The lack of short-timescale variability on LP349−25 on timescales of 10 s or larger is constrained by the observations conducted on 2007 January 12, for 10.7 hr at both 3.6 and 6 cm. This observation duration should have been long enough to discern periodic variability: for $v \sin i \gtrsim 10$ km s^{-1}, the rotation period for a 0.12 $R_{\odot}$ star of mass $\sim$0.09 $M_{\odot}$ (Pont et al. 2005) is $<$10 hr (in which case we should have seen one complete rotation period), and for $v \sin i \gtrsim 20$ km s^{-1}, we should have seen two or more rotation periods. Rotational modulation of the radio emission from ultracool dwarfs is a commonly observed behavior (Hallinan et al. 2006, 2007, 2008), and so its lack in the case of LP349−25 is significant. We note that the greatest constraints on lack of short-term variability come from our C-configuration observation spanning 10.7 hr, but the observation of LP349−25 described by Phan-Bao et al. (2007) lasted 1.7 hr. Expressed as a fraction of the unknown rotation period this span Δt is 1.7 hr/P; taking the upper limit on P to be 10 hr, this observation spanned a fraction of the rotation period $\Delta P/P >$ 0.17. For short periods (2–3 hr), this is a significant fraction of the rotation period, and the lack of variability seen during this observation provides an additional constraint on the lack of rotationally modulated emission for the case of short periods.

The absence of variability in LP 349−25 on timescales comparable to the rotation period of one or both stars imposes spatial constraints. The viewing orientation could explain the lack of variability: if the inclination of the binary system is situated close to pole-on then no modulation of the radio emission is to be expected if either or both dwarfs produces radio emission. However, the preliminary measurement of a substantial $v \sin i$ discussed in Section 2.1 suggests that one or both of the dwarfs may be rapidly rotating, and for a pole-on configuration no rotational broadening of emission lines is expected. However, if the system was not observed at a nearly pole-on configuration, then the pattern of temporal emission would resemble the pulsar behavior seen in other ultracool dwarfs (Hallinan et al. 2006, 2007, 2008). There could be many emitting structures whose properties are uniform and so cause a lack of observed rotational modulation. This would require a high degree of homogeneity of the magnetic structures over the surface of one or both stars. A peculiar arrangement could be obtained between both ultracool dwarfs where both are radio emitting but do so out of phase with each other, so that the total observed radio emission appears to be constant. This seems unlikely, as it would require rather special conditions to occur; namely, the two dwarfs are tidally locked or information can be communicated on timescales <10 s. The separation of the two dwarfs at the discovery epoch was ≈ 1.8 AU, and this distance is too large for tidal locking to occur: the synchronization timescale given by Zahn (1977) is ~ 34 GYr. Finally, a circumbinary radio-emitting structure could be present, but given the separation of the two dwarfs ($\gtrsim 3000\ R_\star$ at the discovery epoch) this is also unlikely.

Since variability is a key factor controlling the observed radio emission from other ultracool dwarfs, we explore some physical constraints imposed by the variability timescales here. Timescales as short as a few minutes have been observed during impulsive bursting behavior (Burgasser & Putman 2005; Berger et al. 2008). We explore the time evolution of the radio emission on short-timescales under the constraints that no emission variability is observed. If the emission is due to singular injection events akin to the isolated bursts seen in other systems, then assuming that the emission region is localized, energy loss can occur through collisional losses in a high-density environment, or radiation losses in a high magnetic field region. The timescale for this energy loss then can be related to the limits on observed variability, to provide a constraint on the plasma environment. The collisional deflection time for a particle of energy $E_{\rm kev}$ is

$$t_c = 9.5 \times 10^7 \frac{E_{\rm kev}}{n_e} \frac{20}{\ln(4.2 \times 10^5 T/\sqrt{n_e})} s \quad (1)$$

(Equation (2.6.20) of Benz 2002), with $E_{\rm kev}$ the particle energy in keV, electron density n_e in cm^{-3}, and temperature T in K; for $T > 10^6$ K and a 10 keV particle to have $t_c < 10$ s requires $n_e \gtrsim 3\times10^8$ cm^{-3}, while $t_c > 10.7$ hr requires $n_e \lesssim 4 \times 10^5$ cm^{-3}. The constraints do not depend tightly on the choice of T. The timescale for radiation loss is

$$t_r = \frac{6.7 \times 10^8}{B^2 \gamma} s \quad (2)$$

(Petrosian 1985) where B is the magnetic field strength in Gauss, γ is the Lorentz factor; for a 10 keV electron, t_r is greater than 10.7 hr for $B \lesssim 130$ G or less than 10 s for $B \gtrsim 10^4$ G. Although we cannot rule out that variability is occurring on timescales less than 10 s, the extreme plasma conditions ($n_e \gtrsim 3\times10^8$ cm^{-3} or $B \gtrsim 10^4$ G) make the scenario of rapid variability on these timescales implausible. Therefore, we consider that the observations constrain the plasma conditions to be either $B \lesssim 130$ G or $n_e \lesssim 4 \times 10^5$ cm^{-3}.

5.2. Constraints from Stability over Long-Timescales

The lack of long-timescale variability on LP349−25 is constrained by the three epochs of flux density measurements at 3.6 cm, and two epochs of measurements at 6 cm. The average flux densities at 3.6 cm are 5% and 30% different comparing the 2005 December/2007 January and 2007 August/2007 January flux density measurements, respectively, while at 6 cm the average flux densities are 6% different. Even in active stars with multiple measurements of "quiescence" outside of any obvious variability, different radio flux densities and spectral indices are obtained (see Figure 3 and discussion in Güdel 2002), revealing differing radio-emitting magnetic configurations. Table 2 of Osten et al. (2004) shows a factor of 15 variation in the average 3.6 cm flux density of the active binary HR 1099, and Caillault et al. (1988) noted that 6 cm detections and upper limits for different epochs of radio observations of BY Draconis variables varied by as much as an order of magnitude. The rotational modulation noted by Lim et al. (1992) of AB Dor's radio emission is only sporadic, indicating a lack of long-term stability or repeatability of the flux density. The well-studied radio-emitting ultracool dwarf TVLM513−46546 also displays different radio emission properties over long-timescales, ranging from variability of quiescent emission (Hallinan et al. 2006) to periodic bursting radio emission (Hallinan et al. 2007) to steady quiescent emission (Berger et al. 2008). The changes in the radio emission properties in the case of both active stars and ultracool dwarfs can be linked to the finite lifetime of the starspots or magnetic structures which are presumed to give rise to the radio emission. Starspots on active stars have lifetimes which depend on their latitude: long-lived spots lying at high latitudes can survive for years (Strassmeier 2002) but starspots at lower latitudes have lifetimes of less than about a month (Hussain 2002). Işik et al. (2007) also showed that starspot lifetime on active stars was longer for larger spots. These trends are due to the competing effects on magnetic flux transport of differential rotation, convection, and meridional flows. The changes in the optical properties of the ultracool dwarf TVLM513-46456 are characterized in one epoch by rotational modulation of isolated starspots (Lane et al. 2007) and in another by rotation of persistent dust clouds (Littlefair et al. 2008), confirming the finite lifetime of magnetic structures in ultracool dwarfs as well. So the stability of the radio-emitting source in LP 349−25 over similar timescales as those during which the radio emission from TVLM513−46546 was observed to change dramatically is unique. This remarkable stability is consistent with similar conditions being the three (two) epochs when 3.6 cm (6 cm) observations were obtained, over timescales of more than a year. This indicates that the magnetic structure giving rise to the radio emission for LP 349−25 lies predominantly at high latitudes, if the same magnetic structure is giving rise to the radio emission in all three epochs. It also suggests that the lifetimes of the magnetic structures are long-lived, or alternatively that there is little variation in the properties of the magnetic structures which form.

5.3. Constraints from Spectral Index

The spectral index measurements of LP 349−25 during the C- and A-configuration epochs described in Section 4.2 are

the same to within 2σ, and consistent to 2σ with a value of 0. For these purposes, we consider this "flat" even though with the same statistical significance the two spectral index measurements are compatible with the range $-0.01 < \alpha < 0.29$. Section 4.2 also described the lack of evidence for changes in the spectral index within the C-configuration observations on timescales greater than 10 s. A primary constraint on the radio emission mechanism from the spectral index is that it does not change significantly. At the most basic level, this indicates that there were no observed changes in optical depth on timescales either within the C-configuration observations (>10 s), or on longer timescales between the two epochs in which both 3.6 and 6 cm observations were obtained (0.6 years).

Optically thin thermal bremsstrahlung naturally produces a flat spectral index (Dulk 1985). In this case, the optical depth is expressed as $\tau_\nu \sim 0.2\, n_e^2 L/\nu^2/T^{3/2}$, where T is the temperature of the thermal plasma, L is the characteristic length scale along the line of sight, and n_e and ν are the electron density and observing frequency, respectively. The brightness temperature $T_b = T\tau$ for $\tau \ll 1$, and the flux density S_ν is

$$S_\nu = \frac{k_B \nu^2}{c^2} T_b \Delta\Omega, \tag{3}$$

where k_B is Boltzmann's constant, c is the speed of light, and $\Delta\Omega$ is the differential solid angle. Writing $\Delta\Omega$ as A/d^2 with A the source area and d the distance to the target, we can express the flux density as a function of the observed temperature and volume emission measure (VEM $= n_e^2 \times A \times L$),

$$S_\nu = 1.4 \times 10^{-54} \frac{\mathrm{VEM}}{\sqrt{T}} \mathrm{Jy} \tag{4}$$

where the VEM has units of cm^{-3} and temperature is in units of K. Thermal bremsstrahlung emission from a chromosphere or corona at temperatures from 10^4 to 10^6 K imply VEMs around 10^{53} cm^{-3} for the observed levels of radio flux density.

As described in Osten et al. (2006), the distribution of spectral indices for a sample of active K and M dwarfs taken from Güdel & Benz (1996) has an average of −0.4 and FWHM of 1.5. The behavior of LP349−25 is consistent with this spread. The interpretation for active stars is that the emission arises from an inhomogeneous source emitting optically thin gyrosynchrotron emission. In the optically thin limit, for a value δ parameterizing the number density distribution of accelerated electron energies ($N(E) \propto E^{-\delta}$), the flux density depends on frequency as $S_\nu \propto \nu^{1.22-0.9\delta}$, so a flat spectrum could be obtained if the spectrum of nonthermal electrons is particularly hard, $\delta \sim 1.3$.

Another possibility to explain a flat spectral index is a hybrid of the above two models, optically thick gyrosynchrotron emission with opacity provided by collisions. This model obtains a flat spectral index for a value δ of 3.6. For this model, a large electron density is required for the collisional opacity to exceed the gyrosynchrotron opacity. For the conditions described in Section 5.1, namely, $T \sim 10^6$ K and $B \lesssim 130$ G, n_e must be $\gtrsim 10^{14}$ cm^{-3} for values of the total nonthermal electron density >1. This is at odds with the restrictions in Section 5.1 necessitating a low electron density ($n_e \leqslant 4 \times 10^5$ cm^{-3}) for the plasma cooling time to be long enough that no variability would have been seen.

5.4. Putting It All Together: Implications for the Radio Emission in LP349−25

The discussion in the above three sections describes temporal and spectral index constraints on the radio emission from LP 349−25. Here, we examine these constraints, together with the upper limits on circular polarization and possible values of brightness temperature, for what they can tell us about the radio emission from this ultracool dwarf binary.

The simplest explanation which fits the lack of variability and flat spectral index observed on LP 349−25 is that the emission arises from optically thin thermal bremsstrahlung radiation distributed uniformly across one or both of the stellar disks. However, this model runs into several problems. If we assume that this material is distributed homogeneously across the disk of one star, with length scale equal to $R_\star$ or smaller, then electron densities in excess of 2.2×10^{11} cm^{-3} are required to produce the VEM determined in Section 5.3. The plasma frequency corresponding to such a density n_e would be $\nu_p \gtrsim 4.2\ (n_e/2.2 \times 10^{11})$ GHz, with n_e in cm^{-3}, and we would expect a cutoff at or below the 6 cm observing frequency. Optically thin radio bremsstrahlung emission would also show up at longer wavelengths as X-ray emission, and given the distance of LP349−25, implies an X-ray flux from 0.2–2.4 keV of $\sim 4 \times 10^{-11}$ erg cm^{-2}, or L_X of 10^{30} erg s^{-1}. This would put LP349−25 in the top 101 brightest X-ray stars within 50 pc (Makarov 2003) and would make the lack of a detection in the *ROSAT* All-Sky Survey, which had sensitivities well below this flux value (down to 10^{-13} erg cm^{-2} s^{-1}; Hünsch et al. 1999) problematic. It would equally well represent a discontinuity with the X-ray behavior of other ultracool dwarfs, which have L_X typically around 10^{26} erg s^{-1} (Stelzer et al. 2006) when they are detected.

The emission from radioactive stars and ultracool dwarfs by extension is usually associated with the presence of enhanced magnetic fields, which naturally leads to gyrosynchrotron or synchrotron emission for incoherent radiation, or cyclotron maser emission for coherent radiation. These mechanisms require accelerated particles, and so the constraints on the plasma environment deduced in Section 4.1 from the lack of aperiodic short-term variability are applicable here. The general gyrosynchrotron model as applied to active stars would require a spatially inhomogeneous source to arrive at the flat spectral index. However, the lack of short-term variability described in Section 4.1 requires that the same emitting region be visible over the one or more rotation periods seen in the C-configuration data. Based on expected lifetimes of starspots seen in active stars and the evidence for epoch-to-epoch changes of radio emission in another well-studied ultracool dwarf, a long-lived polar spot and the binary having a high orbital/rotational inclination are plausible. This would naturally explain both the lack of short-term and long-term variability, as the high inclination would lead to no rotational modulation over the short term, and the similar values of flux density and spectral index are consistent with the same emitting structure producing the observed radio emission. A highly homogeneous source with a hard distribution of electrons would also produce a flat spectral index, as discussed in Section 5.3. Either of these explanations requires that there is little long-term evolution of magnetic structures responsible for producing the radio emission, which is unique among active stars. It is also at odds with the preliminary evidence that one or more of the stars produces a large $v \sin i$ signature discussed in Section 2.1. Gyrosynchtron emission usually arises at frequencies corresponding to harmonic numbers s between 10 and 100 of the electron gyrofrequency, given by $\nu = s\nu_B$, with $\nu_B = 2.8 \times 10^6 B$, B being the magnetic field in the radio-emitting source in Gauss and ν_B in Hz. The ranges of magnetic field strengths derived from the two observing

frequencies is $17 < B < 170$ G for 6 cm emission, and $30 < B < 300$ G for 3.6 cm, which is compatible with the magnetic field strength derived in Section 4.1 to explain the lack of short-term variability. A hybrid collisional/gyrosynchrotron model, although producing a flat spectral index, is difficult to reconcile based on the high electron density required for collisional opacity to exceed gyrosynchrotron opacity. The inferred brightness temperatures, as discussed in Phan-Bao et al. (2007), are not constraining, due to uncertainties in the source size. Research on solar bursts indicates that gyrosynchrotron radiation can be directive (Lee & Gary 2000), although the requirements for lack of periodic variability in this case require that the source be located at high latitudes, with a high inclination, and either isotropic or beamed emission can be accommodated.

A coherent mechanism like electron–cyclotron maser could also be operating to produce the radio emission from LP 349−25. While the intense bursts observed from several ultracool dwarfs have been interpreted using this framework, this is also problematic within the context of the observations and constraints described here. The observed emission shows no net polarization, which could be explained if the emission is intrinsically polarized but becomes depolarized due to propagation and scattering effects. Hallinan et al. (2006) noted that the average emission from TVLM513−46546 was flat, but these measurements were not obtained simultaneously and includes periodic emission, and so it is not clear if the flat spectral index measured from TVLM513−46546 has any bearing on the observed flat spectral index for LP349−25 in the absence of any variability. Cyclotron maser emission at the fundamental or second harmonic is emitted at frequencies $\nu = s\nu_B$ where s is 1 or 2, respectively. A maser operating at the observing frequencies of 4.8 (8.4) GHz requires a magnetic field in the emitting region of 1.7 (3) kG for fundamental emission at 6 (3.6) cm, and 0.86 (1.5) kG for second harmonic emission at the same respective frequencies. Given the constraints on magnetic field strength from lack of variability on short- and long-timescales from Section 5.1, namely, that $B < 130$ G or $B > 10^4$ G, in neither case would a maser would be observable at 3.6 or 6 cm. Plasma conditions must also be favorable for a cyclotron maser to operate, the ratio of plasma frequency to cyclotron frequency, ν_p/ν_B, being less than one. For fundamental or harmonic emission, with the constraints on n_e and B from Section 4.1, this ratio is ~ 0.01, and so is met. There is no general context to explain a particular value of spectral index under electron cyclotron maser emission. Broadband coherent emission as suggested by Hallinan et al. (2006) requires that the radiation be emitted at multiple points in the stellar atmosphere, or arise from relativistic electrons $\Delta\nu/\nu \sim (\gamma - 1)/\gamma$. We can dismiss the latter case because this implies $\gamma \approx 2$, or electrons with kinetic energy >511 keV, which would be much more energetic than have ever been detected from active stars; even discussions of the electron cyclotron maser on the Sun consider particle energies of a few tens of keV (Tang & Wu 2009). In addition, in order for electrons of this energy to retain their energy for timescales longer than 10.7 hr requires plasma environments of $n_e < 10^6$ cm^{-3} and $B < 90$ G to survive against collisional losses and radiative losses, respectively. This is incompatible with the requirement to have the magnetic field in the emitting region be between 0.86 and 3 kG based on identification of the observing frequency with the fundamental or harmonic of the electron gyrofrequency. It is always possible that the maser is continuously resupplied with relativistic particles but this requires that particle acceleration be steady over the long-timescales constrained here (1.6 years), and suggests an even lower magnetic field strength in the source if the particles are to survive against radiative losses. This may necessitate a resupply of relativistic electrons over these long-timescales with no change in intensity or spectral index. Astrophysical sources of particle acceleration are by and large associated with variability, either radio or X-ray synchrotron variability, and indicate stochastic acceleration. Under these conditions, we find the cyclotron maser interpretation of this steady radio emission from LP 349−25 to be problematic, and in light of this we conclude that an incoherent mechanism is most compatible with the observational constraints.

In summary, the variability constraints argue for a high latitude source with a high rotational/orbital inclination in order not to observe any rotationally induced intensity changes. This same source should survive for at least 0.6 yr to explain the similar values of α in two epochs, and requires that there is little evolution of the magnetic configuration that gives rise to the radio emission. Gyrosynchrotron emission from a spatially inhomogeneous or homogeneous source can explain the flat spectral index. The plasma environment must consist of low densities ($n_e \lesssim 4 \times 10^5$ cm^{-3}) and moderate magnetic field strengths ($B < 130$ G) in order that the high-energy electrons not lose energy by collisions or radiation on timescales comparable to those imposed by our C-configuration observations. In contrast, problems are encountered with a cyclotron maser mechanism explanation in key aspects of the observations. Within the context provided by the lifetimes of starspots, and with the expectation that the radio emission arises from a region of enhanced magnetic fields, the constraints imply that a stable polar spot emitting gyrosynchrotron emission may be the origin of the steady radio emission from LP 349−25. Further monitoring of LP 349−25 to determine whether it is variable may help answer other questions about radio emission from ultracool dwarfs, namely, the nature of the unpolarized "steady" radio emission observed outside of highly polarized bursts on other ultracool dwarfs.

Note that the overall detection rates of radio emission for ultracool dwarfs, $\sim 10\%$, are not that different from the optical flare duty cycles of 5%–7% (Reid et al. 1999; Martín & Ardila 2001) and the implied radio duty cycles of $\sim 10\%$ for the transiently emitting object 2M0523. There may be a significant bias in the number of objects which produce detectable levels of radio emission if variability affects the detection rates; potentially more ultracool dwarfs may be capable of producing detectable but transient levels of radio emission than are currently assessed by single epoch surveys. This highlights the need for multiple epoch observations of radio-detected ultracool objects, and probably further monitoring of objects previously undetected in earlier epochs. The recent detection of several unidentified submillijansky radio transients (Bower et al. 2007) suggests that there may be a large reservoir of low-mass or ultracool stellar objects at distances of ≈ 1 kpc producing transient radio emission which can contribute to the rate of radio transients. Further characterizing the behavior of nearby low-mass and ultracool dwarfs is therefore necessary to be disentangle a stellar component from this unknown source population.

6. CONCLUSIONS

Our investigation of the radio emission from three ultracool dwarfs yields useful constraints from only one. The temporal

and multi-frequency radio observations of LP 349−25 suggest that the radio-emitting structures are located at a high latitude on one of the stars, and that the rotational and orbital axes have a high inclination with respect to our line of sight, in order to explain the lack of variation associated with orbital or rotational modulation. This is potentially at odds with the preliminary determination of the $v \sin i$ of the system. The absence of transient or aperiodic variability over short-timescales also constrains the plasma conditions which must be present, in order that high-energy particles not lose their energy through collisions or radiative losses. The similar flux density values and spectral indices returned from epochs 0.6 years apart are consistent with a long-lived magnetic structure giving rise to the emission. We explore the implications for the radio-emitting mechanism, and rule out a thermal source. Gyrosynchrotron emission from an inhomogeneous or homogeneous source can explain the flat spectral index and is compatible with the limits imposed on the plasma environment from short-timescale constraints. An electron–cyclotron maser is not compatible with the plasma constraints. In terms of its observational properties and the implications provided thereby for the radio emission mechanism, LP 349−25 is unique among ultracool dwarfs in exhibiting an incoherent mechanism, and suggests that the mixed behavior of active stars at radio wavelengths, exhibiting one or both of gyrosynchrotron and a coherent emission mechanism, can survive to the substellar boundary. Temporal constraints on long-timescales imply that there is little long-term evolution of magnetic structures, an important result for the magnetic fields only recently established to be present in ultracool dwarfs. Further monitoring will confirm whether LP349−25 is truly unique in its steady multi-frequency emissions, and interferometric observations at higher angular resolution are needed to determine whether one or both dwarfs contributes to the total radio emission. Both steady and transient radio emission have been presented in this paper, and our conclusions support continued monitoring of all radio-detected ultracool dwarfs in order to elucidate further the nature of radio emission near the substellar boundary.

This paper represents the results of VLA programs AO205, AO214, and AO223. Support for this work was provided by NASA through Hubble Fellowship grant HF-01189.01 awarded by the Space Telescope Science Institute, which is operated by the Association of Universities for Research in Astronomy, Inc. for NASA, under contract NAS5-26555.

REFERENCES

Antonova, A., Doyle, J. G., Hallinan, G., Golden, A., & Koen, C. 2007, A&A, 472, 257
Basri, G., & Reiners, A. 2006, AJ, 132, 663
Benz, A. (ed.) 2002, Astrophysics and Space Science Library, Vol. 279, Plasma Astrophysics (2nd ed; Dordrecht: Kluwer)
Benz, A. O., & Güdel, M. 1994, A&A, 285, 621
Berger, E. 2002, ApJ, 572, 503
Berger, E. 2006, ApJ, 648, 629
Berger, E., et al. 2001, Nature, 410, 338
Berger, E., et al. 2005, ApJ, 627, 960
Berger, E., et al. 2008, ApJ, 673, 1080
Bouy, H., et al. 2004, A&A, 423, 341
Bower, G. C., Saul, D., Bloom, J. S., Bolatto, A., Filippenko, A. V., Foley, R. J., & Perley, D. 2007, ApJ, 666, 346
Burgasser, A. J., & Putman, M. E. 2005, ApJ, 626, 486
Burgasser, A. J., Reid, I. N., Siegler, N., Close, L., Allen, P., Lowrance, P., & Gizis, J. 2007, in Protostars and Planets V, ed. B. Reipurth, D. Jewitt, & K. Keil (Tucson, AZ: Univ. Arizona Press), 427
Caillault, J.-P., Drake, S., & Florkowski, D. 1988, AJ, 95, 887
Close, L. M., Siegler, N., Potter, D., Brandner, W., & Liebert, J. 2002, ApJ, 567, L53
Cruz, K. L., Reid, I. N., Liebert, J., Kirkpatrick, J. D., & Lowrance, P. J. 2003, AJ, 126, 2421
Dulk, G. A. 1985, ARA&A, 23, 169
Fleming, T. A., Giampapa, M. S., Schmitt, J. H. M. M., & Bookbinder, J. A. 1993, ApJ, 410, 387
Forveille, T., et al. 2005, A&A, 435, L5
Fuhrmeister, B., Schmitt, J. H. M. M., & Hauschildt, P. H. 2005, A&A, 439, 1137
Gatewood, G., Boss, A., Weinberger, A. J., Thompson, I., Majewski, S., Patterson, R., & Coban, L. 2005, BAAS, 37, 1269
Gizis, J. E., Monet, D. G., Reid, I. N., Kirkpatrick, J. D., Liebert, J., & Williams, R. J. 2000, AJ, 120, 1085
Güdel, M. 2002, ARA&A, 40, 217
Güdel, M., & Benz, A. O. 1993, ApJ, 405, L63
Güdel, M., & Benz, A. O. 1996, in ASP Conf. Ser. 93, Radio Emission from the Stars and the Sun, ed. A. R. Taylor & J. M. Paredes (San Francisco, CA: ASP), 303
Hallinan, G., Antonova, A., Doyle, J. G., Bourke, S., Brisken, W. F., & Golden, A. 2006, ApJ, 653, 690
Hallinan, G., Antonova, A., Doyle, J. G., Bourke, S., Lane, C., & Golden, A. 2008, ApJ, 684, 644
Hallinan, G., et al. 2007, ApJ, 663, L25
Hawley, S. L., Gizis, J. E., & Reid, I. N. 1996, AJ, 112, 2799
Hünsch, M., Schmitt, J. H. M. M., Sterzik, M. F., & Voges, W. 1999, A&AS, 135, 319
Hussain, G. A. J. 2002, Astron. Nachr., 323, 349
Işik, E., Schüssler, M., & Solanki, S. K. 2007, A&A, 464, 1049
Koen, C. 2005, MNRAS, 360, 1132
Lane, C., et al. 2007, ApJ, 668, L163
Lee, J., & Gary, D. E. 2000, ApJ, 543, 457
Lim, J., Nelson, G. J., Castro, C., Kilkenny, D., & van Wyk, F. 1992, ApJ, 388, L27
Littlefair, S. P., Dhillon, V. S., Marsh, T. R., Shahbaz, T., Martin, E. L., & Copperwheat, C. 2008, MNRAS, 391, L88
Makarov, V. V. 2003, AJ, 126, 1996
Martín, E. L., & Ardila, D. R. 2001, AJ, 121, 2758
Mohanty, S., & Basri, G. 2003, ApJ, 583, 451
Mohanty, S., Basri, G., Shu, F., Allard, F., & Chabrier, G. 2002, ApJ, 571, 469
Osten, R. 2007, in Proc. Bursts, Pulses and Flickering: Wide Field Monitoring of the Dynamic Radio Sky (Dynamic2007), 5
Osten, R. A., Hawley, S. L., Bastian, T. S., & Reid, I. N. 2006, ApJ, 637, 518
Osten, R. A., et al. 2004, ApJS, 153, 317
Petrosian, V. 1985, ApJ, 299, 987
Phan-Bao, N., Osten, R. A., Lim, J., Martín, E. L., & Ho, P. T. P. 2007, ApJ, 658, 553
Pont, F., Melo, C. H. F., Bouchy, F., Udry, S., Queloz, D., Mayor, M., & Santos, N. C. 2005, A&A, 433, L21
Pradel, N., Charlot, P., & Lestrade, J.-F. 2006, A&A, 452, 1099
Reid, I. N., & Cruz, K. L. 2002, AJ, 123, 2806
Reid, I. N., Kirkpatrick, J. D., Gizis, J. E., & Liebert, J. 1999, ApJ, 527, L105
Reiners, A., & Basri, G. 2007, ApJ, 656, 1121
Schmitt, J. H. M. M., Fleming, T. A., & Giampapa, M. S. 1995, ApJ, 450, 392
Stelzer, B., Micela, G., Flaccomio, E., Neuhäuser, R., & Jayawardhana, R. 2006, A&A, 448, 293
Strassmeier, K. G. 2002, Astron. Nachr., 323, 309
Tang, J. F., & Wu, D. J. 2009, A&A, 493, 623
West, A. A., et al. 2004, AJ, 128, 426
Zahn, J.-P. 1977, A&A, 57, 383